Journal of Materials Chemistry A

High thermoelectric and mechanical performance in highly dense Cu2-xS bulks prepared by a melt-solidification technique

Journal:	*Journal of Materials Chemistry A*
Manuscript ID:	TA-COM-03-2015-001667.R1
Article Type:	Communication
Date Submitted by the Author:	26-Mar-2015
Complete List of Authors:	zhao, lanling; Institute for Superconducting and Electronic Materials, AIIM Wang, Xiaolin; uow, Fei, Frank; uow, Wang, Jiyang; State Key Lab. of Crystal Materials, Cheng, Zhenxiang; uow, Dou, Shixue; uow, Wang, Jun; uow, Snyder, G.; Northwestern University,

Journal Name

RSCPublishing

COMMUNICATION

High thermoelectric and mechanical performance in highly dense $Cu_{2-x}S$ bulks prepared by a melt-solidification technique

Cite this: DOI: 10.1039/xoxxoooooox

Received ooth January 2012,
Accepted ooth January 2012

DOI: 10.1039/xoxxoooooox

www.rsc.org/

Lanling Zhao[a], Xiaolin Wang[a], Frank Yun Fei[a], Jiyang Wang[b], Zhenxiang Cheng[a], Shixue Dou[a], Jun Wang[a], and G. Jeffrey Snyder[c]*

Highly dense $Cu_{2-x}S$ bulks, fabricated by a melt-solidification technique, show high thermoelectric performance with zT of ~ 1.9 at 970 K. The $Cu_{2-x}S$ bulks show good thermal heat flow and diffusivity stability, and they exhibit excellent mechanical properties, with hardness of ~ 1 GPa. Density functional theory calculations indicate that $Cu_{2-x}S$ is an intrinsic p-type conductor.

1 Introduction

High temperature thermoelectric materials have received great attention due to their crucial roles in direct energy conversion between heat and electricity, based on the Seebeck effect[1] and Peltier effect[2]. It is well known that the energy conversion efficiency for thermoelectric devices at a temperature T can be estimated by the dimensionless figure-of-merit (zT), defined as $zT = S^2T\sigma/\kappa$, where S, T, σ, and κ are the Seebeck coefficient, absolute temperature, electrical conductivity, and total thermal conductivity, respectively.[3-7] Apparently, high zT values can be achieved with concurrent high S and σ values, and low κ values.

Recently, it has been reported that hot-pressed $Cu_{2-x}S$ polycrystalline bulks show high thermoelectric performance with the highest zT values on record, ~ 1.7 at 1000 K.[8, 9] Furthermore, $Cu_{2-x}S$ consists of copper and sulfur, both of which are naturally abundant and non-toxic. Therefore, $Cu_{2-x}S$ should be one promising high temperature thermoelectric materials. It should be noted that the polycrystalline bulks were generally fabricated by the hot pressing method using spark plasma sintering (SPS) systems under high temperature and high pressure. This approach requires costly instruments and high electrical current for SPS, and may lead to Cu migration[10], which is disadvantageous for the large-scale fabrication of homogeneous thermoelectric materials. Therefore, it is favourable to find one time and energy efficient method to fabricate highly dense $Cu_{2-x}S$ samples. Furthermore, good stability for the thermoelectric properties such as electrical conductivity, Seebeck coefficient, and thermal conductivity are crucial for the practical applications of thermoelectric materials. Hence, it is essential to do repeated heating and cooling measurements to test the thermoelectric stability of the $Cu_{2-x}S$ compound.

In addition, mechanical stress caused by the good contact between the thermoelectric modules and the heat source, and thermal stress, induced by the temperature gradient between the hot and cold sides, coexist in the interior of thermoelectric devices, which can reduce the reliability of thermoelectric modules.[11-13] Therefore, besides the high zT values, thermoelectric materials should also have good mechanical properties, and it is important to investigate the mechanical properties of the fabricated $Cu_{2-x}S$ samples.

It should be noted that the high-temperature α-phase $Cu_{2-x}S$ has the same cubic crystal structure (space group: $Fm\bar{3}m$)[14-16] and superionic transport[17] as $Cu_{2-x}Se$[18, 19], which makes this family of compounds distinct from other high temperature thermoelectric materials and leads to additional considerations for their use[20]. It has been reported that hot-pressed $Cu_{2-x}S$ bulks show lower electrical conductivity than hot-pressed $Cu_{2-x}Se$ bulks[9, 19], indicating that there may be some differences in doping or in their electronic band structures due to the differences in the lattice parameter and ionic radius of Se^{2-} and S^{2-}. Therefore, it is desirable to investigate the electronic band structure for the $Cu_{2-x}S$ system.

Herein, we report the successful fabrication of highly dense Cu_2S and $Cu_{1.97}S$ bulks through a melt-solidification technique. The fabricated $Cu_{1.97}S$ bulks show zT values as high as ~ 1.9 at 973 K, which confirms the reported high zT result and is somewhat higher than for the hot-pressed polycrystalline $Cu_{1.97}S$ bulks. Moreover, the fabricated Cu_2S and $Cu_{1.97}S$ samples show good thermal stability during repeated heating and cooling processes, and they exhibit excellent mechanical performance with the $Cu_{1.97}S$ having a much higher Vickers hardness of ~ 1.0 GPa compared to PbTe[21], Bi_2Te_3[22], and PbSe[23] polycrystalline bulks. Density functional theory (DFT) calculations of the high temperature α-phase $Cu_{2-x}S$ reveal that copper deficient $Cu_{2-x}S$ compounds are intrinsic p-type conductors with similar band structure but shifted Fermi level compared to the stoichiometric Cu_2S.

2 Experimental

Highly dense $Cu_{2-x}S$polycrystalline bulks were fabricated by a melt-solidification technique. A mixture of Cu and S powders in the molar ratio 2-x : 1 (x = 0 and 0.03) was pressed into pellets and sealed in evacuated quartz tubes, before being heated to 400 ºC for 1-5 hours with a heating rate of 5 ºC/min, and then heated to ~ 1150 ºC for 1-2 hours with a heating rate of 5 ºC/min, followed by a furnace cooling to room temperature. The obtained bulks were shaped into disks with dimensions of Φ10 mm × 1 mm for the thermal diffusivity measurements. After the measurements, the same sample disks were cut into rectangular bars for measurements of the electrical conductivity and Seebeck coefficient.

X-ray diffraction (XRD) patterns and field emission scanning electron microscope (FE-SEM) images were collected on GBC MMA and JEOL JSM-7500FA systems, respectively. The electrical conductivity and Seebeck coefficient were measured simultaneously in a helium atmosphere in the temperature range from 400 to 973 K using a RZ2001i system. The thermal diffusivity (D) was measured by the laser flash method (LINSEIS LFA 1000), and the specific heat (C_p) was determined by differential scanning calorimetry (Mettler Toledo TGA/DSC 1). The sample density (*dd*) was determined by the Archimedes method. The thermal conductivity (κ) was calculated by $\kappa = D \times C_p \times dd$. Vickers hardness of the as-prepared samples was measured at different locations employing the Duramin 70 Vickers hardness tester applying a load of 0.1 N.

First principles calculations were performed using density functional theory (DFT) implemented by the Cambridge Serial Total Energy Package (CASTEP) package[24]. The generalized gradient approximation (GGA)[25] was used in this calculation, with parameterization by the Perdew-Burke-Ernzerhof (PBE)[26] and ultra-soft pseudopotentials. The plane wave cut-off energy was set at 400 eV. A 4×4×4 Monkhorst-Pack k-point mesh, with a Brillouin zone path of ΓXWLΓK of the primitive cell, was employed for the band structure calculations. The total and partial density of states of Cu_2S and copper deficient $Cu_{1.875}S$ were calculated on a 2×2×2 super-cell of the primitive cell.

3 Results and discussion

Fig. 1 shows the X-ray diffraction patterns and typical field emission scanning electron microscope cross-sectional image for the theCu_2S and $Cu_{1.97}S$ bulks fabricated by a melt-solidification technique. The results indicate that all the fabricated bulks are single phase and crystallized in the orthorhombic structure (PDF No. 23-961). Furthermore, the bulks are composed of highly dense and micro-scale grains without any visible voids or porosity.

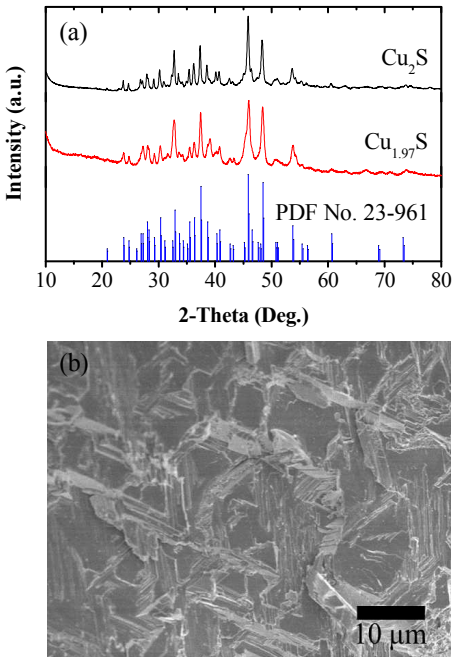

Fig. 1 (a) X-ray diffraction patterns for theCu_2S and $Cu_{1.97}S$ bulks fabricated by a melt-solidification technique, and for standard low temperature β-phase Cu_2S (PDF No. 23-961), and (b) Typicalfield emission scanning electron microscope cross-sectional image of the melted-solidified bulks.

Fig. 2 shows the temperature dependence of the electrical conductivity, Seebeck coefficient, thermal conductivity, and dimensionless figure-of-merit for the fabricated Cu_2S and $Cu_{1.97}S$ bulks in the temperature range from 400 K to 1000 K. The electrical conductivity for the high temperature α-phase $Cu_{1.97}S$ bulks decreases as the temperature increases, showing the typical electrical

conductivity behavior of metallic or heavily doped semiconducting materials, with values between 185 and 120 $S \cdot cm^{-1}$ over a wide temperature range from 700 to 1000 K. On the other hand, the Cu_2S bulks have much smaller electrical conductivity over the whole measured temperature range compared to the $Cu_{1.97}S$ bulks, with the highest value ~ 30 $S \cdot cm^{-1}$ at 973 K. The Cu_2S bulks have a much higher Seebeck coefficient than $Cu_{1.97}S$ from 400 to 1000 K, with the highest values being ~ 240 $\mu V \cdot K^{-1}$ for $Cu_{1.97}S$ and ~ 370 $\mu V \cdot K^{-1}$ for Cu_2S, respectively. The above data reveals that the $Cu_{1.97}S$ should have a higher power factor than the Cu_2S, and the temperature dependence of the power factor is shown in Fig. S1†. The temperature dependence of the specific heat displayed in Fig. S2† indicates that both samples have two phase transitions at around 350 - 400 K and 600 - 750 K. The thermal conductivity displayed in Fig. 2c indicates that both the Cu_2S and the $Cu_{1.97}S$ bulks have low κ values between 0.5 and 0.3 $W \cdot m^{-1} \cdot K^{-1}$ in the temperature range from 400 to 1000 K. The low thermal conductivity may come from the liquid-like behavior of copper ions in the rigid face-centered cubic, fcc, sublattice constituted by the S atoms and the low average speed of sound[9]. The zT values for the Cu_2S and $Cu_{1.97}S$ bulks shown in Fig. 2d demonstrate that the total thermoelectric performance is very sensitive to the copper deficiency, with zT over 1.0 at T > 700 K and as high as 1.9 at 973 K for the $Cu_{1.97}S$, and zT of ~ 1.0 at 973 K for the Cu_2S. Furthermore, in the temperature range from 700 to 1000 K, the Cu_2S and $Cu_{1.97}S$ bulks fabricated by the melt-solidification technique confirm the high thermoelectric performance of $Cu_{2-x}S$ with perhaps even higher zT values compared to the SPS hot-pressed samples[9], which could be due to better optimization of the carrier concentration via the copper deficiency.

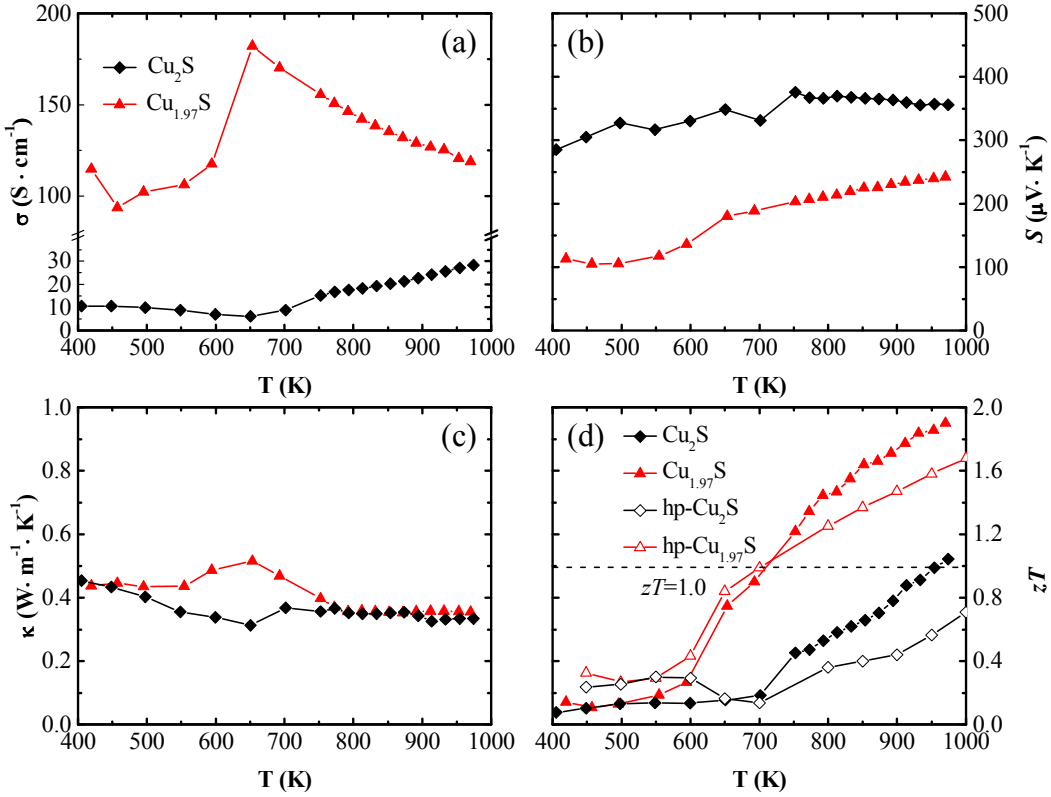

Fig.2 Temperature dependence of the thermoelectric properties for the fabricated Cu_2S and $Cu_{1.97}S$ polycrystalline bulks: (a) electrical conductivity (σ), (b) Seebeck coefficient (S), (c) thermal conductivity (κ), and (d) dimensionless figure-of-merit (zT). The reproduced zT values for hot-pressed polycrystalline samples (labelled as hp-Cu_2S and hp-$Cu_{1.97}S$[9]) are also shown in Fig. 2d.

The electrical and thermal stability are quite essential for the practical applications of thermoelectric materials. Therefore, we repeated the electrical conductivity, Seebeck coefficient and thermal diffusivity measurements several times for the melt-solidified Cu_2S and $Cu_{1.97}S$ samples in the temperature range from 400 to 1000 K, to test whether they are stable or not.

Fig. 4 shows the the temperature dependence of the thermal diffusivity, electrical conductivity (σ), Seebeck coefficient (S), and power factor (PF) for the fabricated Cu_2S and $Cu_{1.97}S$ polycrystalline samples. Additionally, the differential scanning calorimeter (DSC) thermal response measurements plots for the fabricated $Cu_{1.97}S$ sample are also displayed in Fig. S3†. Both the temperature dependent thermal diffusivity and heat flow show good reproducibility, and these results indicate that the fabricated Cu_2S and $Cu_{1.97}S$ bulks are thermally stable during the repeated heating and cooling processes. The elelcrical conductivity and Seebeck coefficient for the Cu_2S and $Cu_{1.97}S$ samples, however, exhibit poor stability under the concurrent of high temperature and electrical field with repeated heating and cooling treatments. The electrical conductivity decreases with

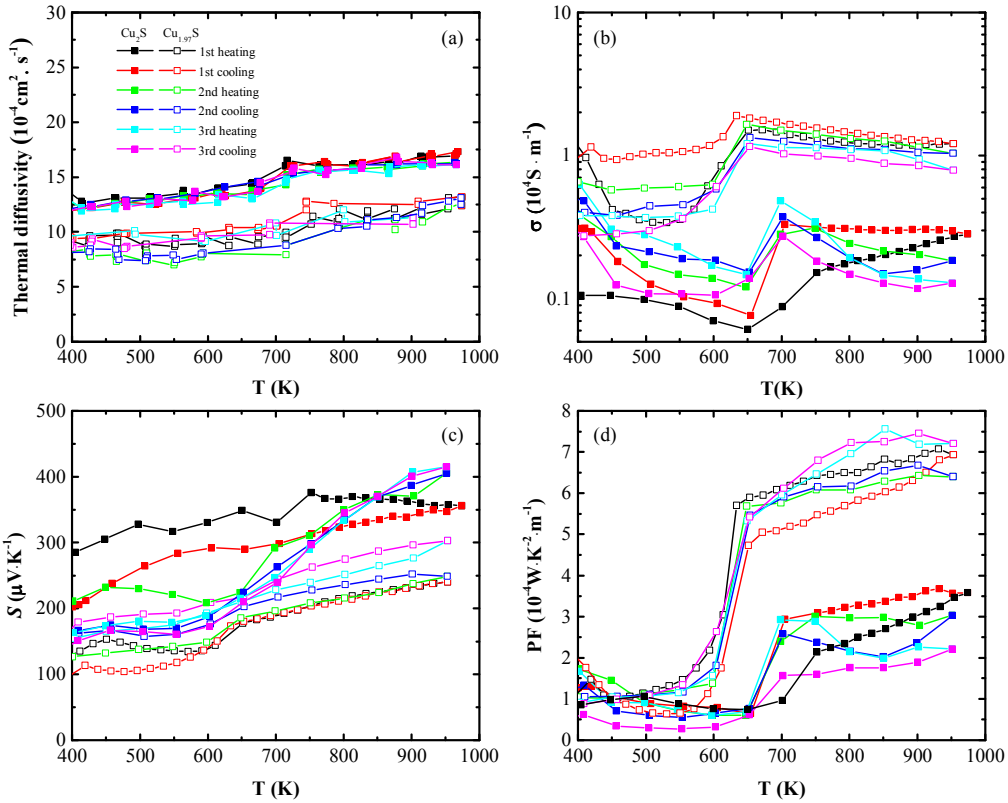

Fig. 3 Temperature dependence of the thermoelectric properties for the fabricated Cu_2S and $Cu_{1.97}S$ polycrystalline bulks: (a) thermal diffusivity, (b) electrical conductivity (σ), (c) Seebeck coefficient (S), and (d) power factor (PF).

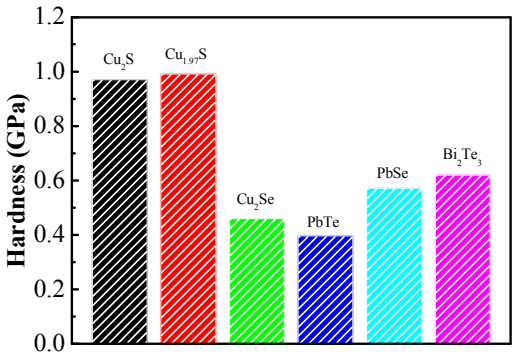

Fig. 4 Vickers hardness values of the fabricated Cu_2S and $Cu_{1.97}S$ bulks. The hardness values of polycrystalline Bi_2Te_3, PbTe, PbSe, and Cu_2Se bulks are also provided for comparison.

the increasing times of heating and cooling processes, while the Seebeck coefficient shows the opposite trend with enhanced values. The calculated power factor for the fabricated Cu_2S and $Cu_{1.97}S$ bulks, especially for the $Cu_{1.97}S$, shows much better stability than that of the electrical conductivity and Seebeck coefficient, thanks to the interaction between them.

This poor reproducibility for the electrical conductivity, Sebbeck coefficient as well as the power factor for the Cu_2S and $Cu_{1.97}S$ samples can be ascribed to several factors. It might be related to the superionic conductivity of this compound, the copper ions could move from one side of the sample to the other side upon the application of an electrical field. Additionally, the evaporation of sulfur during the measurements can also lead to the poor reproducibility of elelctrical conductivity and Seebeck coefficient.[29] These problems might can be restained by decreasing the applied elelctrical field for measurements, doping approaches that can weaken the drift of copper ions, and increasing the pressure of inert gases in the measurement chamber to supress the evaporation. It should be noted that the stable thermal properties, such as heat flow and thermal diffusivity, and ehanced seebeck coefficient after repeated heating and cooling processess, could make this compound find potentail applications in other thermal related areas and sensor applications.

Fig. 4 shows the Vickers hardness values of the Cu_2S and $Cu_{1.97}S$ polycrystalline bulks. The Vickers hardness values of several other thermoelectric materials are also presented for comparison. It was reported that hot-pressed polycrystalline Bi_2Te_3[27], PbTe[28], and PbSe[23] bulks show hardness of around 0.62, 0.40, and 0.60 GPa, respectively. Compared to the $Cu_{2-x}Se$ polycrystalline bulks having hardness of around 0.42 GPa, the Cu_2S and $Cu_{1.97}S$ bulks exhibit much higher hardness, with values of ~ 0.97 GPa for the Cu_2S and ~ 1.0 GPa for the $Cu_{1.97}S$, respectively.

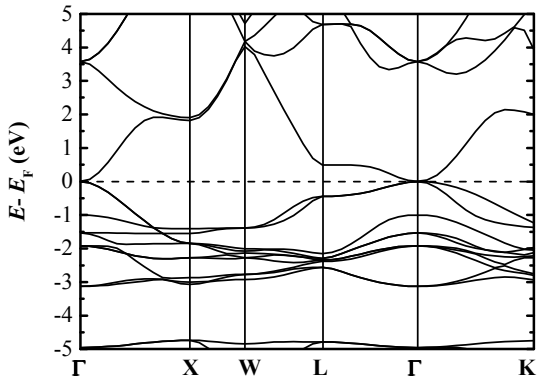

Fig.5 Calculated electronic band structures for the stoichiometric Cu_2S.

Band structure calculations enable us to gain insight into the electronic states near the Fermi level (E_F) as well as the charge carrier types in the system. Fig.5 shows the calculated electronic band structures for the high temperature cubic phase of the stoichiometric Cu_2S. The calculations predict that Cu_2S will be a small-band-gap semiconductor. The calculated band gap is essentially zero at the Γ point, but it is well known that the DFT method often underestimates the gap.

Fig.6 shows the calculated total and partial density of states (DOS) for the stoichiometric Cu_2S and copper deficient $Cu_{1.875}S$. It reveals that the valence bands consist of three regions: a lower region between 12 and 16 eV below the E_F, which is mainly constituted by S 3s states, a middle region between 4 and 8 eV below the E_F, which is a mixture of Cu 3p, 3d, and 4s states, and S 3p states, and an upper region between the E_F and -4 eV, which mostly consists of Cu 3d states, even though the S 3p states also contribute to this region.

For the stoichiometric Cu_2S, the calculated partial and total DOS is in good agreement with the electronic band structure calculation results, further evidence that the stoichiometric Cu_2S is a small-band-gap semiconductor. As to the copper deficient $Cu_{1.875}S$, the Cu 3d states and S 3p states of the middle region, belonging to the valence bands, penetrate into E_F. This explains well why the copper deficient $Cu_{2-x}S$ is a p-type conductor and why its conductivity is higher than that of the stoichiometric Cu_2S from experimental observations.

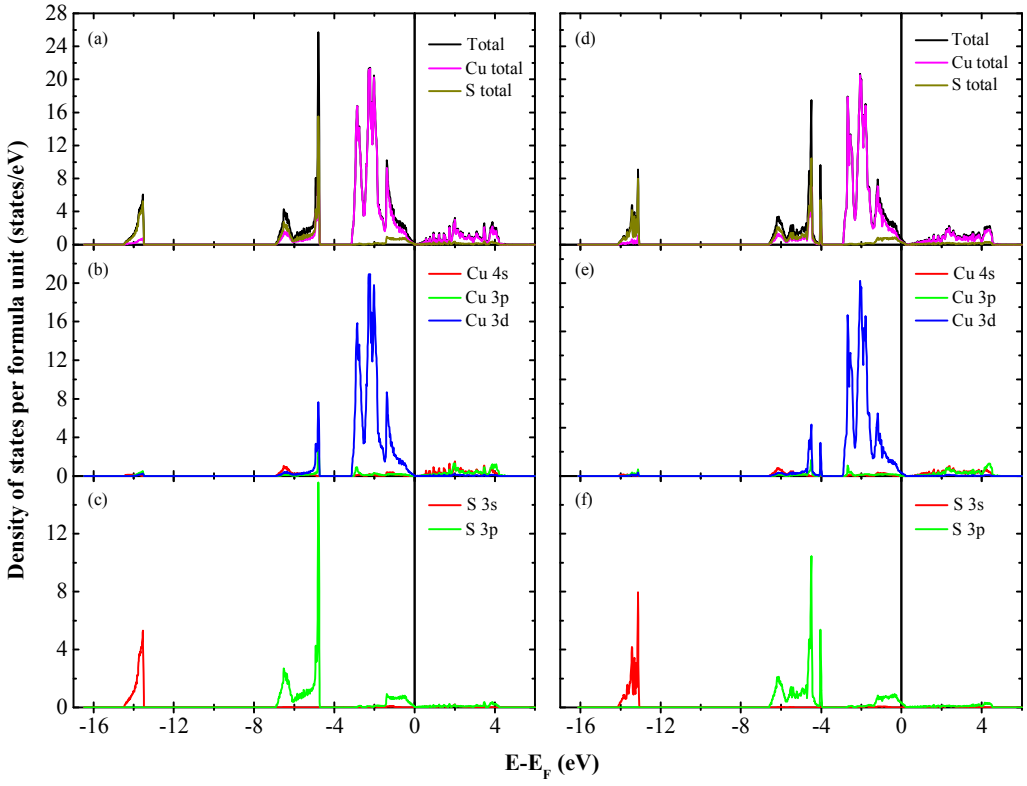

Fig. 6 Calculated total and partial density-of-states (DOS) for the stoichiometric Cu_2S (left) and copper deficient $Cu_{1.875}S$ (right) using density functional theory.

4 Conclusions

In summary, our results indicate that the melt-solidification technique works well for the fabrication of highly dense Cu_2S and $Cu_{1.97}S$ polycrystalline bulks. The fabricated $Cu_{1.97}S$ bulks show excellent thermoelectric performance, with zT as high as ~1.9 at 973 K, and good mechanical properties with a Vickers hardness of ~ 1.0 GPa. Moreover, both the synthesized Cu_2S and $Cu_{1.97}S$ show quite good repeatibility for the thermal diffusivity during the repeated heating and cooling processes, while they exhibit poor reproducibility for the electrical conductivity, Seebcek

coefficient and power factor under the concurrent of high temperature and electrical field. Density functional theory calculations reveal that stoichiometric Cu_2S is a small-band-gap semiconductor, and copper deficiency makes the copper deficient $Cu_{2-x}S$ to be an intrinsic *p*-type conductor.

Acknowledgements

X.L.W. acknowledges support for this work from the Australian Research Council (ARC) through an ARC Discovery Project (DP 130102956) and an ARC Professorial Future Fellowship Project (FT 130100778). L.L.Z. is grateful to the China Scholarship Council (CSC) for providing her PhD scholarship. G.J.S. acknowledges support from the U.S. Department of Energy (DOE EFRC S3TEC).

Notes and references

[a]Spintronic and Electronic Materials Group, Institute for Superconducting and Electronic Materials, Australian Institute for Innovative Materials, University of Wollongong, North Wollongong, 2500, Australia
[b]Institute for Crystal Materials,Shandong University, Jinan, 250100, People's Republic of China
[c]Northwestern University,Materials Science and Engineering, Evanston, Illinois 60208, USA

†Electronic Supplementary Information (ESI) available: Temperature dependence of power factor (PF) for the fabricated Cu_2S and $Cu_{1.97}S$ bulks (Fig. S1); temperature dependence of the specific heat for the fabricated Cu_2S and $Cu_{1.97}S$ (Fig. S2); differential scanning calorimeter thermal response plots for the fabricated $Cu_{1.97}S$ bulks (Fig. S3); ideal version of unit cell and primitive cell for the high temperature α-phase Cu_2S (Fig. S4); and X-ray diffraction patterns for the polycrystalline pellets used for the thermal diffusion measurements (Fig. S5).
See DOI: 10.1039/c000000x/

1. T. Geballe and G. Hull, *Phys. Review*, 1954, **94**, 1134-1140.
2. T. C. Harman, J. H. Cahn and M. J. Logan, *J. Appl. Phys*, 1959, **30**, 1351.
3. C. J. Vineis, A. Shakouri, A. Majumdar and M. G. Kanatzidis, *Adv. Mater.*, 2010, **22**, 3970-3980.
4. P. Jood, R. J. Mehta, Y. Zhang, G. Peleckis, X. Wang, R. W. Siegel, T. Borca-Tasciuc, S. X. Dou and G. Ramanath, *Nano Lett.*, 2011, **11**, 4337-4342.
5. W. Liu, X. Yan, G. Chen and Z. Ren, *Nano Energy*, 2012, **1**, 42-56.
6. M. Zebarjadi, K. Esfarjani, M. S. Dresselhaus, Z. F. Ren and G. Chen, *Energ. Environ. Sci.*, 2012, **5**, 5147.
7. W. G. Zeier, Y. Pei, G. Pomrehn, T. Day, N. Heinz, C. P. Heinrich, G. J. Snyder and W. Tremel, *J. Am. Chem. Soc.*, 2013, **135**, 726-732.
8. Z. H. Ge, B. P. Zhang, Y. X. Chen, Z. X. Yu, Y. Liu and J. F. Li, *Chem.Comm.*, 2011, **47**, 12697-12699.
9. Y. He, T. Day, T. Zhang, H. Liu, X. Shi, L. Chen and G. J. Snyder, *Adv. Mater.*, 2014, **26**, 3974-3978.
10. H. Yin, M. Christensen, N. Lock and B. B. Iversen, *Appl. Phys. Lett.*, 2012, **101**, 043901.
11. Yi Ma, Qing Hao, Bed Poudel, Yucheng Lan, Bo Yu, Dezhi Wang, Gang Chen and Z. Ren,*Nano Lett.*, 2008, **8**, 2580-2584.
12. A. C. Kallel, G. Roux and C. L. Martin, *Mater. Sci. Eng., A*, 2013, **564**, 65-70.
13. K. Ueno, A. Yamamoto, T. Noguchi, T. Inoue, S. Sodeoka and H. Obara, *J. Alloy. Compd.*, 2005, **388**, 118-121.
14. D. J. L. Chakrabarti, D. E., *Bul. Alloy. Phase Diagr.*, 1983, **4**, 254-271.
15. J. William R. Cook, *Solid State Chem.*, 1972, 703-712.
16. J. Howard T. Evans, *Am. Mineral.*, 1981, **66**, 807-818.
17. E. Hirahara, *J. Phys. Soc. Jpn.*, 1951, **6**, 422-427.
18. B. Yu, W. Liu, S. Chen, H. Wang, H. Wang, G. Chen and Z. Ren, *Nano Energy*, 2012, **1**, 472-478.
19. H. Liu, X. Shi, F. Xu, L. Zhang, W. Zhang, L. Chen, Q. Li, C. Uher, T. Day and G. J. Snyder, *Nature Mater.*, 2012, **11**, 422-425.
20. D. R. Brown, T. Day, T. Caillat and G. J. Snyder, *J. Electron Mater.*, 2013, **42**, 2014-2019.
21. Y. Gelbstein, Z. Dashevsky and M. P. Dariel, *J. Appl. Phys.*, 2008, **104**, 033702.
22. G. Li, K. R. Gadelrab, T. Souier, P. L. Potapov, G. Chen and M. Chiesa, *Nanotechnology*, 2012, **23**, 065703.
23. W. B. W. M. S. DARROW, R. ROY, *J. Mater. Sci.*, 1969, 313-319.
24. S. J. Clark, M. D. Segall, C. J. Pickard, P. J. Hasnip, M. I. J. Probert, K. Refson and M. C. Payne, *Z. Kristallogr.*, 2005, **220**.
25. P. Hohenberg and W. Kohn, *Physical Review*, 1964, **136**, B864-B871.
26. J. P. Perdew, K. Burke and M. Ernzerhof, *Phys. Rev. Lett.*, 1996, **77**, 3865-3868.
27. L.-D. Zhao, B.-P. Zhang, J.-F. Li, M. Zhou, W.-S. Liu and J. Liu, *J. Alloy. Compd.*, 2008, **455**, 259-264.
28. Y. Gelbstein, G. Gotesman, Y. Lishzinker, Z. Dashevsky and M. P. Dariel, *Scripta Mater.*, 2008, **58**, 251-254.
29. G. Dennler, R. Chmielowski, S. Jacob, F. Capet, P. Roussel, S. Zastrow, K. Nielsch, I. Opahle, and G. K. H. Madsen, Adv. Energy Mater., 2014, **4**, 1301581.
30. Y. Takagiwa, Y. Pei, G. Pomrehn and G. Jeffrey Snyder, *APL. Mater.*, 2013, **1**, 011101.

